Organic Electronics 11 (2010) 1516–1522

Contents lists available at ScienceDirect

Organic Electronics

journal homepage: www.elsevier.com/locate/orgel

Letter

High efficiency polymer solar cells via sequential inkjet-printing of PEDOT:PSS and P3HT:PCBM inks with additives

Seung Hun Eom [a,b], Hanok Park [a], S.H. Mujawar [a], Sung Cheol Yoon [c], Seok-Soon Kim [d], Seok-In Na [e], Seok-Ju Kang [f], Dongyoon Khim [f], Dong-Yu Kim [f], Soo-Hyoung Lee [a,*]

[a] School of Semiconductor and Chemical Engineering, Chonbuk National University, Jeonju 561-756, Republic of Korea
[b] Korea Printed Electronics Center, Korea Electronics Technology Institute, Jeonju 561-844, Republic of Korea
[c] Advanced Materials Division, Korea Research Institute of Chemical Technology, Daejeon 305-600, Republic of Korea
[d] Department of Nano and Chemical Engineering, Kunsan National University, Kunsan 751-701, Republic of Korea
[e] Korea Institute of Science Technology (KIST), Wanju-gun, Jeollabuk-do 565-902, Republic of Korea
[f] Heeger Center for Advanced Materials, Department of Materials Science and Engineering, Gwangju Institute of Science and Technology (GIST), Gwangju 500-712, Republic of Korea

ARTICLE INFO

Article history:
Received 14 April 2010
Received in revised form 1 June 2010
Accepted 12 June 2010
Available online 22 June 2010

Keywords:
Polymer solar cell
Inkjet-printing
P3HT:PCBM
Active layer
Ink additives

ABSTRACT

Highly efficient and cost-effective polymer solar cells (PSCs) based poly(3-hexylthiophene) (P3HT) and 1-(3-methoxycarbonyl)-propyl-1-phenyl-(6,6)C61 (PCBM) have been fabricated by inkjet-printing with various additives. All solution-processed layers in the solar cells—a poly(3,4-ethylenedioxythiophene):poly(styrenesulfonate) (PEDOT:PSS) layer and a photoactive layer based on P3HT and PCBM with additives—were inkjet-printed. The device performance is strongly influenced by the addition of high boiling point additives in the photoactive ink with chlorobenzene (CB) solvent. The morphology, optoelectronic properties, and overall solar cell performance of the devices were dramatically affected by additives, such as 1,8 octanedithiol (ODT), o-dichlorobenzene (ODCB) and chloronaphthalene (Cl-naph). A device fabricated from ink formulated with ODT exhibited the best overall performance with power conversion efficiency (PCE) of 3.71%.

In the last decade, increasing concern about global warming has led to an intense search for cost-effective alternative energy sources, such as photovoltaics [1–3]. The need to develop inexpensive renewable energy sources has stimulated scientific research into efficient, low cost photovoltaic devices. Existing commercial silicon-based (i.e., inorganic) solar cells have limited use because of expensive and complicated manufacturing processes involving clean rooms and vacuum chambers. Solar cells based on organic semiconductors have become a promising alternative to inorganic photovoltaics due to their low weight, low cost, easy processing, and flexibility, when compared to traditional silicon solar cells [4,5]. Efforts have been made to improve organic solar performance using new materials, novel structures, and new techniques for mass production [6,7].

Among the organic photovoltaic fabrication techniques, inkjet-printing is emerging as a key process that enables digital production technology for solar cell manufacturing. When compared to spin-coating and other conventional printing techniques, inkjet-printing has the advantages of providing a large area, site specific deposition and a non-contact conformal deposition with a minimal loss of material [8]. Combining the inkjet-printing process with the use of flexible substrates has the potential to significantly reduce manufacturing costs by eliminating the patterning process and allowing for a mass production technique, such as roll-to-roll fabrication.

The formulation of an optimized printing ink with a high performance and long storage lifetime is an essential

* Corresponding author. Tel.: +82 63 270 2435; fax: +82 63 270 2306.
E-mail addresses: shlee66@jbnu.ac.kr, shlee66@chonbuk.ac.kr (S.-H. Lee).

1566-1199/$ - see front matter © 2010 Elsevier B.V. All rights reserved.
doi:10.1016/j.orgel.2010.06.007

element in the development of inkjet-printing-based solar cells. In an earlier report, we have demonstrated the use of ZnO as a buffer layer for the inkjet-printing of a silver cathode in a polymer solar cell [9]. We have also reported on the performance of bulk heterojunction polymer solar cells fabricated with an inkjet-printed poly(3,4-ethylenedioxythiophene):poly(styrenesulfonate) (PEDOT:PSS) layer. The morphology and electrical properties of the inkjet-printed PEDOT:PSS layer, as well as the overall device performance, were dramatically affected by the ink formulations containing additives, such as glycerol and a surfactant [10].

Employing a spin-coated P3HT:PCBM active layer, several research groups have reported on the formation of a phase separated morphology with crystalline P3HT and PCBM domains inside the active layer of bulk-heterojunction solar cells. Such a morphology has been achieved by use of an appropriate solvent with a specific boiling point for precise control over the evaporation rate [11,3,12], reducing the drying speed of the spin-coated films [13–15], melting of the bilayers [16], thermal annealing of the fabricated films with or without an applied external voltage [17–19], and using chemical additives [20–22]. Few efforts have been made to fabricate inkjet-printed bulk-heterojunction solar cells. Brabec et al. recently reported the solar cell devices fabricated by inkjet-printing P3HT:PCBM inks formulated with various solvent mixtures on doctor-bladed PEDOT:PSS layer [23–25]. Aernouts et al. also reported the device performance of P3HT:PCBM active layer with high boiling point (b.p.) solvent mixtures for reducing coffee-ring effect [26]. However, to the best of our knowledge, no researchers have reported on efficient polymer solar cells fabricated by inkjet-printing both the PEDOT:PSS layer and the P3HT:PCBM active layer.

In this work, we report on highly efficient and cost-effective inkjet-printed PSCs based on P3HT and PCBM inks containing various additives. All solution-processed solar cell layers—a hole transporting layer of PEDOT:PSS and a photoactive layer based on P3HT and PCBM with various additives—were inkjet-printed. The conditions of the inkjet-printed PEDOT:PSS layers were optimized based on the results of our previous study [10]. Changes in the morphology, optoelectronic properties, and overall device performance that resulted from the addition of various high b.p. additives, such as 1,8 octanedithiol (ODT), o-dichlorobenzence (ODCB), and 1-chloronaphthalene (Cl-naph), to chlorobenzene (CB) solvents were investigated.

Regioregular poly(3-hexylthiophene) (P3HT) as an electron donor and [6,6]-phenyl-C61 butyric acid methylester (PCBM) as an electron acceptor were purchased from Rieke metals and Nano-C, respectively. Poly(3,4-ethylenedioxythiophene):poly-(styrene sulfonic acid) (PEDOT:PSS) was purchased from Bayer (Baytron P AI 4083). Several high b.p. additives, such as ODT, ODCB, and Cl-naph, were obtained from Sigma-Aldrich and used as-received. In the present study, the configuration of the polymer solar cell devices was indium tin oxide (ITO)/PEDOT:PSS/active layer of P3HT:PCBM/LiF-Al. Patterned ITO glass was cleaned with chloroform, acetone, and isopropyl alcohol using an ultrasonication method. The ITO was then subject to an O2-plasma treatment. To PEDOT:PSS inks for inkjet-printing, PEDOT:PSS was mixed with additives of glycerol (0.431) and ethylene glycol butyl ether (EGBE, 0.014). Details regarding the optimization of the additive concentrations to obtain the best PEDOT:PSS layer can be found in our previous report [10]. After a solvent cleaning, the PEDOT:PSS inks were deposited on the ITO substrates using an inkjet-printing (UJ2100, Unijet, Korea) technique. The films were then dried for 20 min at 140 °C.

To optimize the parameters for the inkjet-printing of an active layer, blends (inks) of P3HT:PCBM (1:0.7, 2 wt%) in CB with different high b.p. additives of ODT, ODCB, and Cl-naph were prepared (details are given in Table 1). These inks were printed on top of the PEDOT:PSS layers by the same printer used for the PEDOT:PSS deposition. Temperatures of inkjet-printer head and substrate were kept as 26C. The printed films were then dried for 1 h at room temperature in a nitrogen atmosphere. By varying the ink concentrations and the printing speed, the optimum thickness of the P3HT:PCBM layers was found to be 150 nm. Thermal evaporation was used to deposit a LiF layer (0.5 nm thickness) on the active layer. To complete the device, an Al layer (150 nm thickness) was evaporated on top of the LiF layer. All evaporations were performed under vacuum (10-6 torr). Each completed device was encapsulated so as to measure the solar cell performance.

The current density–voltage (J–V) characteristics of the solar cell devices in the dark and under white light illumination were measured with an AM 1.5G solar simulator (300 W, Newport, USA) calibrated to 100 mW/cm2 with a standard PV reference cell (a 2 × 2 cm monocrystalline silicon solar cell, calibrated at NREL, Colorado, USA) using a Keithley 2400 source-measure unit. The open circuit voltage (Voc), short circuit current density (Jsc), fill factor (FF), and power conversion efficiency (PCE) were calculated from the J-V curves. The incident photon to collected electron efficiency (IPCE) of the devices was measured with a commercial photomodulation spectroscopic setup that included a xenon lamp (Oriel), iris diaphragms, and an AM 1.5 filter. In order to avoid an underestimation of the area of the devices due to cross-conduction through

Table 1
Formulation details of the P3HT:PCBM inks containing different high b.p. additives.

Inks	P3HT:PCBM (1:0.7)	CB (b.p = 132 °C)	ODT (b.p = 269 °C)		ODCB (b.p = 179 °C)		Cl-naph (b.p = 259 °C)	
	g	ml	ml	vol.%	ml	vol.%	ml	vol.%
1	0.2	10	-	-	-	-	-	-
2	0.2	10	0.5	5	-	-	-	-
3	0.2	10	-	-	0.5	5	-	-
4	0.2	10	-	-	-	-	0.5	5

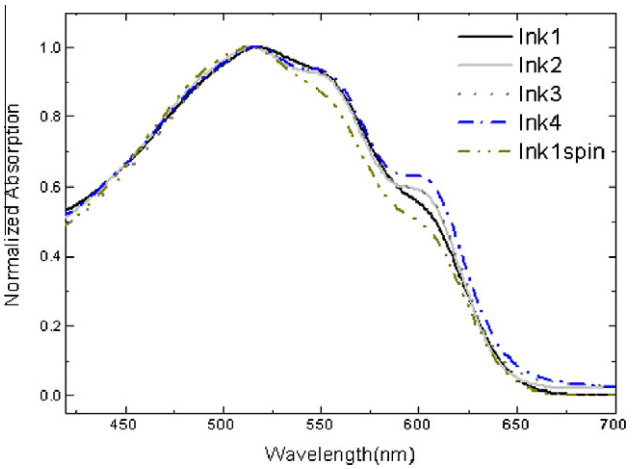

Fig. 1. UV–Vis absorption spectra of the inkjet-printed active layers fabricated from different inks.

the highly conducting PEDOT:PSS used in this study, a black mask fitted to the active area (3×3 mm) of the devices was employed [27–29]. The surface morphology and absorption spectra of the inkjet-printed active layers were analyzed using atomic force microscopy (AFM, Nanoscope IV, Multimode) and UV–Vis spectroscopy (JASCO, V-670), respectively. The crystallinity of the P3HT was examined with X-ray diffractometry (XRD, Rigaku, with a Cu Kα source). All characterizations were performed at room temperature.

Shown in Fig. 1 are the optical absorption spectra as a function of wavelength for the inkjet-printed active layers containing different additives; the reference film was fabricated by spin-coating. The film spin-coated with ink1, formulated with CB and no additives, exhibits an absorption spectrum with a maximum centered at 509 nm with two indistinct shoulders at 544 and 595 nm. For the inkjet-printed films from ink2 contained 5 vol% ODT, ink3 contained 5 vol% ODCB, and ink4 contained 5 vol% Cl-naph, a red shift with relatively wide absorption in the longer wavelength region was clearly observed; maxima were located at 513 nm, and two pronounced vibronic peaks emerged at 552 and 602 nm [30,31]. As the film thickness is identical for all four films, the observed red shift is evidence of improved π–π^* transition absorption due to the increased conjugation length of polymer chains. The increased conjugation length of the polymer chains was caused by a reduction in the density of conformational defects. The addition of a moderate amount of high b.p. additives to the CB allows for the slow evaporation of the solvent and hence, leads to enhanced P3HT crystallinity. The improvement in the crystallinity is generally observed in the case of post-annealed P3HT-based polymer solar cells [4,19]. As such, the inkjet-printing method with modified inks containing high b.p. additives can act as a substitute for crucial post-annealing treatments. When compared to spin-coated devices, inkjet-printed solar cells fabricated with inks containing additives have improved crystallinity and better light harvesting properties over a wider spectral region. Consequently, the inkjet-printed solar cells are expected to exhibit improved photovoltaic performance.

The XRD results for the inkjet-printed active layer films fabricated with different inks are shown in Fig. 2. The peak intensity at $2\theta \approx 5.3$, which corresponds to the interchain spacing associated with the interdigitated alkyl chain in P3HT [4,32], was more enhanced in the films fabricated with high b.p. additives (inks 2–4). The maximum peak intensity was observed in the film fabricated with ink4, which contained the Cl-naph additive. These results are in agreement with the trends observed for the vibronic peak in the UV absorption spectra shown in Fig. 1. In addition, when high b.p. additives are added to the inks (inks 2–4), the 2θ angle of (100) of films is moved to higher angle: 5.24 for ink 1, 5.30 for ink 2 and 3, and 5.42 for ink 4. According to the Bragg's equation ($n\lambda = 2d \sin\theta$, where n, λ, d, and θ denote the order of diffraction, wavelength of an X-ray beam, interlayer spacing, and Bragg peak position, respectively) [33,34], a interlayer spacing of films fabricated with high b.p. additives (inks 2–4) is less than that of film prepared from pure P3HT:PCBM ink (ink1). It indicates that modification of inks with high b.p. additives induces closer P3HT chains, resulting in the lower resistance to the hopping of charge carriers.

Morphology is one of the key factors that affect the performance of bulk-heterojunction solar cells. To investigate the effects of additives and inkjet-printing on the morphology, the surface of the active layer films was imaged using an atomic force microscope (AFM). Shown in Fig. 3 are the AFM images of the inkjet-printed active layers fabricated with different inks; the reference cell fabricated from spin-coating is shown for comparison. From the AFM images ($100 \times 100\mu$m), it is clear that the morphology is greatly influenced by the addition of different high b.p. additives to the CB solvent. The film prepared with ink1 (CB with no additives) possesses an rms roughness of 64 nm, which is very high when compared to the films fabricated from inks 2–4. Such a high rms roughness may be due to the high evaporation rate of the CB. If the rate of evaporation of the solvent is high, then there may not be

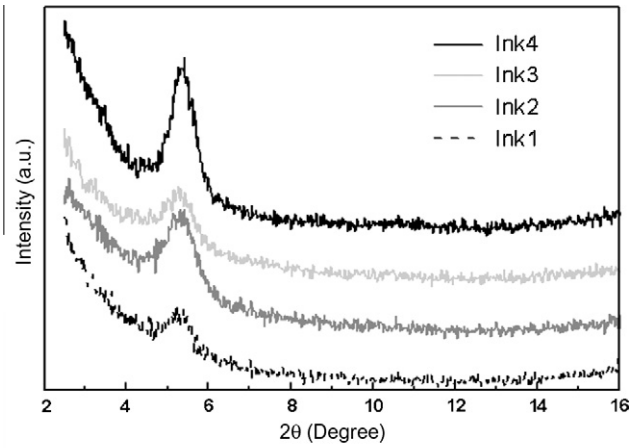

Fig. 2. XRD spectra of the inkjet-printed active layers fabricated from different inks.

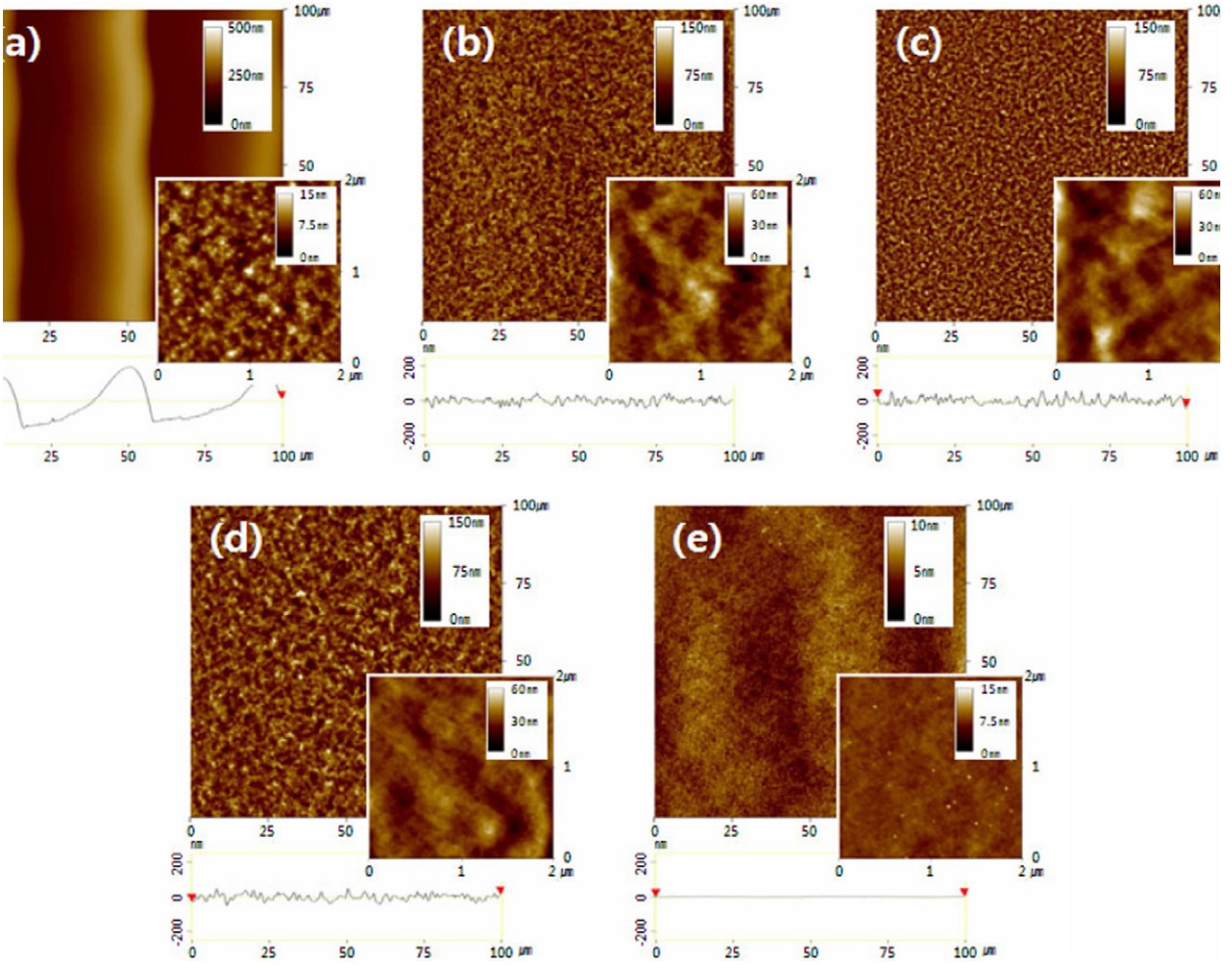

Fig. 3. AFM images of the P3HT:PCBM active layers fabricated from different inks: inkjet-printed (a) ink1 (b) ink2 (c) ink 3 (d) ink 4 and (e) spin-coated ink1.

sufficient time for self organization of the blended P3HT polymer molecules. This would result in a coating with a rough and uneven surface. On the other hand, the films from ink2, ink3, and ink4 possess moderate rms roughnesses on the order of 17.7, 20.9, and 17.9 nm, respectively. As stated above, ink2, ink3, and ink4 contain high b.p.

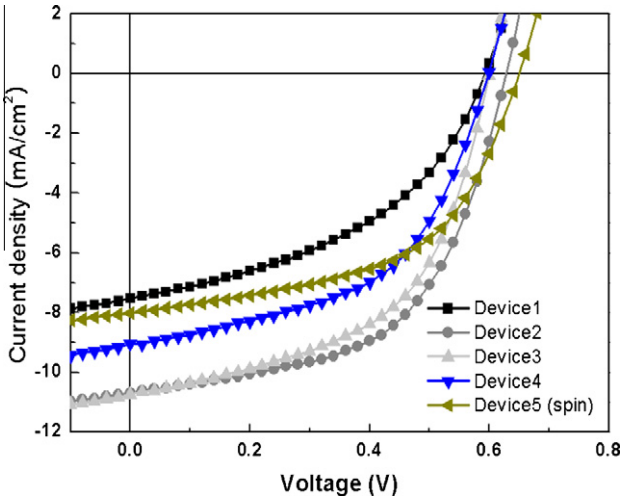

Fig. 4. J–V characteristics of the solar cell devices with P3HT:PCBM active layers fabricated from different inks.

additives of 5 vol% ODT, 5 vol% ODCB, and 5 vol% Cl-naph, respectively. The observed decrease in the rms roughness values can be attributed to the low evaporation rates of the high b.p. additives. These high b.p. additives allow for a controlled evaporation and sufficient time for self organization to occur. The additives may also provide enhanced wettability of the P3HT:PCBM inks on the PEDOT:PSS layer, leading to an active layer with a uniform film morphology and reducing the coffee-ring effect [35]. In general, it can be concluded that the addition of high b.p. additives offers control over the morphology of the P3HT and PCBM domains in the inkjet-printed active layer. The reference device (ink1) fabricated by spin-coating possessed a very low rms roughness of 1 nm, which may be due to the high spinning rate used in this study. However, when compared to the inkjet-printed films, the film spin-coated from ink1 exhibited a homogeneous morphology with no significant phase separation. The AFM images in the inset of Fig. 3 ($2 \times 2\mu m$ scan size) more clearly reveal that the films inkjet-printed from inks 2–4 show more distinct nanoscale phase separation than in the spin-coated film. The increased phase separation is a result of polymer self organization and leads to an increase in device efficiency. However, it should be noted that the film inkjet-printed from ink4 exhibits an undesirably large degree of phase separation between the P3HT and PCBM (the average size of the domains is greater than 100 nm), which may result in the restriction of charge transport.

To directly evaluate the effect of high b.p. additives on the overall device performance, the J–V characteristics of all the solar cells were measured under illumination with a solar simulator. Shown in Fig. 4 are the J–V plots for all devices; the calculated values of the solar cell parameters are summarized in Table 2. As clearly evident in Fig. 4, the device fabricated with ink1 (device 1) without any additives exhibits very poor performance with a PCE ~1.9% resulting relatively lower Voc, Jsc and FF than other devices. The observed low device performance may be due to poor P3HT crystallinity, relatively weak absorption in the longer wavelength region and undesirable film morphology (see Figs. 1–3) that serve to restrict the transport of the photo-generated charges towards the electrodes. In contrast, the device fabricated with ink2 (device 2) exhibited the best performance with a PCE of ~3.7% and an FF that increased up to ~56%. Such a result was believed to arise from a higher level of P3HT crystallinity and distinct nanoscaled phase separation morphology. These factors, in turn, led to a lower serial resistance and defect-free contact with the metal cathode. The device prepared with ink3 (device 3) had a Jsc of ~10.7 mA/cm2, which was similar to the Jsc from device 2. However, a slight reduction in the Voc to ~0.6 V was observed in device3, which led to a decrease in the PCE to ~3.4%. The device prepared with ink4 (device 4) yielded a PCE of 2.83% and lower Jsc and Voc values than those found for devices 2–3. This may due to a low photo current, which is in turn attributed to limitations in the charge transport and collection by the large phase separated morphology (see the AFM images in Fig. 3). The exact reasons of lower Voc are not clearly reported yet even though several efforts have been made to fabricate inkjet-printed bulk-heterojunction solar cells with active layer of P3HT:PCBM [24,25]. In organic solar cells, the Voc is generally governed by the energy difference between the highest occupied molecular orbital (HOMO) of the donor and the lowest unoccupied molecular orbital (LUMO) of acceptor [36]. An increase in the conjugation length due to strong chain interactions improves the crystallinity with long wavelength absorption. Such a scenario leads to an improved Jsc, but may cause a reduction in the Voc in the devices 1–4 fabricated by

Table 2
Summary of the solar cell device performance for the different P3HT:PCBM active layers containing different additives.

Devices with inks	V_{oc} (V)	J_{sc} (mA/cm^2)	FF (%)	PCE (%)
Device 1 (ink 1)	0.593	7.53	44.25	1.97
Device 2 (ink 2)	0.628	10.68	55.27	3.71
Device 3 (ink 3)	0.600	10.73	53.28	3.43
Device 4 (ink 4)	0.599	9.49	52.23	2.83
Device 5 (ink 1, spin)	0.650	8.02	53.58	2.79

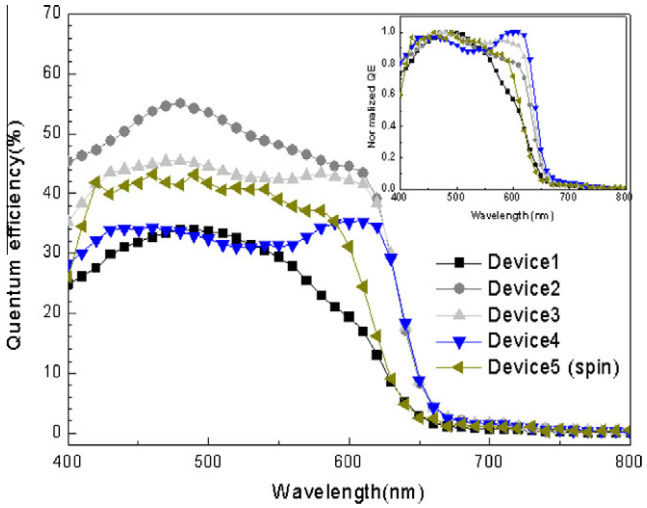

Fig. 5. The IPCE spectra of solar cell devices with P3HT:PCBM active layers fabricated from different inks.

inkjet-printing, especially in device 4 showing a high crystallinity (see Fig. 2). Device5, fabricated by spin-coating with ink1, exhibited a PCE of 2.79%, which was lower than that found in the inkjet-printed devices (devices 2–4) even though it shows a higher Voc and comparable FF than inkjet-printed devices (devices 2–4). Such a low PCE may due to poor P3HT crystallinity and weak absorption in the longer wavelength region, resulting a lower Jsc, for the active layer fabricated by the spin-coating method (see Figs. 1 and 2).

Shown in Fig. 5 are the plots of the IPCE measured for all of the devices. The dependence of the IPCE on the post-production treatment has been reported by several groups; IPCE values of up to 70–80% have been achieved [19,37–40]. Devices 2–4, which were inkjet-printed from inks 2–4 with additives, showed significant IPCE improvement in the longer wavelength region, when compared to device 1 (no additives) and device 5 (spin-coated from ink1) (see the inset of Fig. 5). While device 5 possessed a low rms roughness, it exhibited a low IPCE of 50%, when compared to devices 2–3 due to its low optical absorption in the longer wavelength region. A maximum IPCE of up to 55% was measured with device 2. Device 1, fabricated from ink1, containing no high b.p. additive, exhibited the lowest IPCE of about 30%. This may due to its low crystallinity and relatively weak absorption in the longer wavelength region. Device 4, made with ink4, exhibited a relatively low IPCE value even though it displayed good absorption at longer wavelengths. Such a scenario may be due to the limited charge transport that is related to the large degree of phase separation. The attained IPCE results are in good agreement with the trends observed in the optical absorption spectra and the device performance data shown in Figs. 1 and 4. The profound improvement in the IPCE with the addition of different additives is believed to increase both the optical absorption and the charge transport, as well as reduce recombination losses due to improvements in crystallinity and surface morphology. Therefore, it can be concluded that inkjet-printing provides a two-fold improvement in the overall solar cell performance, i.e. efficient light harvesting by improved P3HT crystallinity and enhanced charge transport and offering a better surface morphology for the top metal contact.

Bulk heterojunction polymer solar cells have been prepared with an inkjet-printed active layer of P3HT:PCBM and a PEDOT:PSS layer. For an optimum ink formulation, different high b.p. additives, such as ODT, ODCB, and Cl-naph were added to CB. The addition of high b.p. additives has greatly influenced the morphology, the optical and electrical properties, and the solar cell performance of the devices. The devices fabricated from inks formulated with high b.p. additives have exhibited improved device performance, when compared to the devices prepared without additives. Such behavior was due to optimum film morphology, improved light absorption properties, and reduced recombination losses due to an improved crystallinity and charge transport. The inkjet-printed device with an active layer of P3HT:PCBM containing the high b.p. additive ODT and a modified PEDOT:PSS layer has demonstrated the best solar cell performance with a PCE of ~3.7% and an IPCE of ~55%.

Acknowledgments

This work was supported by Ministry of Commerce, Industry and Energy (MOCIE) under Grant No. 200701-0041. This research was also financially supported by the Ministry of Education, Science Technology (MEST) and Korea Industrial Technology Foundation (KOTEF) through the Human Resource Training Project for Regional Innovation.

References

[1] N.S. Sariciftci, L. Smilowitz, A.J. Heeger, F. Wudl, Science 258 (1992) 1474.
[2] J.J.M. Halls, C.A. Walsh, N.C. Greenham, E.A. Marseglia, R.H. Friend, S.C. Moratti, A.B. Holmes, Nature 376 (1995) 498.

[3] G. Yu, J. Gao, J.C. Hummelen, F. Wudl, A.J. Heeger, Science 270 (1995) 1789.
[4] W. Ma, C. Yang, X. Gong, K. Lee, A.J. Heeger, Adv. Funct. Mater. 15 (2005) 1617.
[5] Y. Kim, S. Cook, S.M. Tuladhar, S.A. Choulis, J. Nelson, J.R. Durrant, D.D.C. Bradley, M. Giles, I. Mcculloch, C.-S. Ha, M. Ree, Nat. Mater. 5 (2006) 197.
[6] M. Svensson, F. Zhang, S.C. Veenstra, W.J.H. Verhees, J.C. Hummelen, J.M. Kroon, O. Inganãs, M.R. Andersson, Adv. Mater. (Weinheim, Ger.) 15 (2003) 988.
[7] M. Granström, K. Petritsch, A.C. Arias, A. Lux, M.R. Andersson, R.H. Friend, Nature (London) 395 (1998) 257.
[8] R.W. Vest, K.F. Teng, Metallization of solar cells with ink jet printing and silver metallo-organic inks, IEEE transactions on components, hybrids and manufacturing technology 11 (3) (1988) 291–297.
[9] S.H. Eom, S. Senthilarasua, P. Uthirakumar, C.H. Hong, Y.S. Lee, J. Lim, S.C. Yoon, C. Lee, S.H. Lee, Solar Energy Materials and Solar Cells 92 (2008) 564.
[10] S.H. Eom, S. Senthilarasua, P. Uthirakumar, S.C. Yoon, J. Lim, C. Lee, H.S. Lim, J. Lee, S.H. Lee, Organic Electronics 10 (2009) 536.
[11] S.E. Shaheen, C.J. Brabec, N.S. Sariciftci, Appl. Phys. Lett. 78 (2001) 841.
[12] Y. Kim, S.A. Choulis, J. Nelson, D.D.C. Bradley, S. Cook, R. Durrant, Appl. Phys. Lett. 86 (2005) 063502.
[13] G. Li, V. Shrotriya, J. Huang, Y. Yao, T. Moriarty, K. Emery, Y. Yang, Nat. Mater. 4 (2005) 864.
[14] P. Vanlaeke, G. Vanhoyland, T. Aernouts, D. Cheyns, C. Deibel, J. Manca, P. Heremans, J. Poortmans, Thin Solid Films 511 (2006) 358.
[15] V.D. Mihailetchi, H. Xie, B. de Boer, L.M. Popescu, J.C. Hummelen, P.W.M. Blom, L.J.A. Koster, Appl. Phys. Lett. 89 (2006) 012107.
[16] K. Kim, J. Liu, D.L. Carroll, Appl. Phys. Lett. 88 (2006) 181911.
[17] H. Hoppe, N.S. Sariciftci, J. Mater. Chem. 16 (2006) 45.
[18] H. Hoppe, N.S. Sariciftci, J. Mater. Res. 19 (7) (2004) 1924.
[19] F. Padinger, R.S. Rittberger, N.S. Sariciftci, Adv. Funct. Mater. 13 (2003) 85.
[20] J. Peet, J.Y. Kim, N.E. Coates, W.L. Ma, D. Moses, A.J. Heeger, G.C. Bazan, Nat. Mater. 6 (2007) 497.
[21] K.J. Lee, W.L. Ma, C.J. Brabec, J. Yuen, J.S. Moon, J.Y. Kim, K. Lee, Guillermo C. Bazan, A.J. Heeger, J. Am. Chem. Soc. 130 (2008) 3619.
[22] F.-C. Chen, H.-C. Tseng, C.-J. Ko, Appl. Phys. Lett. 92 (2008) 103316.
[23] C.N. Hoth, S.A. Choulis, P. Schilinsky, C.J. Brabec, Adv. Mater. 19 (2007) 3973.
[24] C.N. Hoth, P. Schilinsky, S.A. Choulis, C.J. Brabec, Nano Lett. 8 (2008) 2806.
[25] C.N. Hoth, S.A. Choulis, P. Schilinsky, C.J. Brabec, J. Mater. Chem. 19 (2009) 5398.
[26] T. Aernouts, T. Aleksandrov, C. Girotto, J. Genoe, J. Poortmans, Appl. Phys. Lett. 92 (2008) 033306.
[27] J. Park, H.-J. Koo, B. Yoo, K. Yoo, K. Kim, W. Choi, N.-G. Park, Sol. Energy Mater. Sol. Cells 91 (2007) 1749.
[28] A. Cravino, P. Schilinsky, C.J. Brabec, Adv. Funct. Mater. 17 (2007) 3906.
[29] M.-S. Kim, M.-G. Kang, L.J. Guo, J.S. Kim, Appl. Phys. Lett. 92 (2008) 133301.
[30] G. Li, Y. Yao, H. Yang, V. Shrotriya, G. Yang, Y. Yang, Adv. Func. Mater. 17 (2007) 1636.
[31] T.-F. Guo, T.-C. Wen, G.L. Pakhomov, X.-G. Chin, S.-H. Liou, P.-H. Yeh, C.-H. Yang, Thin solid film 516 (2008) 3138.
[32] S. Kim, S. Na, S. Kang, D. Kim, Sol. Energy Mater. Sol. Cells 94 (2010) 171.
[33] A. Zen, J. Pflaum, S. Hirschmann, W. Zhuang, F. Jaiser, U. Asawapirom, J.P. Rabe, U. Scherf, D. Neher, Adv. Func. Mater. 14 (2004) 757.
[34] T. Erb, U. Zhokhavets, G. Gobsch, S. Raleva, B. Stühn, P. Schilinsky, C. Waldauf, C.J. Brabec, Adv. Funct. Mater. 15 (2005) 1193.
[35] M. Singh, H.M. Haverinen, P. Dhagat, C.E. Jabbour, Adv. Mater. 22 (2010) 673.
[36] M.C. Scharber, D. Mühlbacher, M. Koppe, Patrick Denk, C. Waldauf, A.J. Heeger, C.J. Brabec, Adv. Mater. 18 (2006) 789.
[37] D. Chirvase, J. Parisi, J.C. Hummelen, V. Dyakonov, Nanotechnology 15 (2004) 1317.
[38] G. Li, V. Shrotriya, Y. Yao, Y. Yang, J. Appl. Phys. 98 (2005) 043704.
[39] I. Riedel, V. Dyakonov, Phys. Status Solidi (A), Phys. Appl. Res. 201 (6) (2004) 1332.
[40] M.R. Reyes, K. Kim, D.L. Carroll, Appl. Phys. Lett. 87 (2005) 083506.